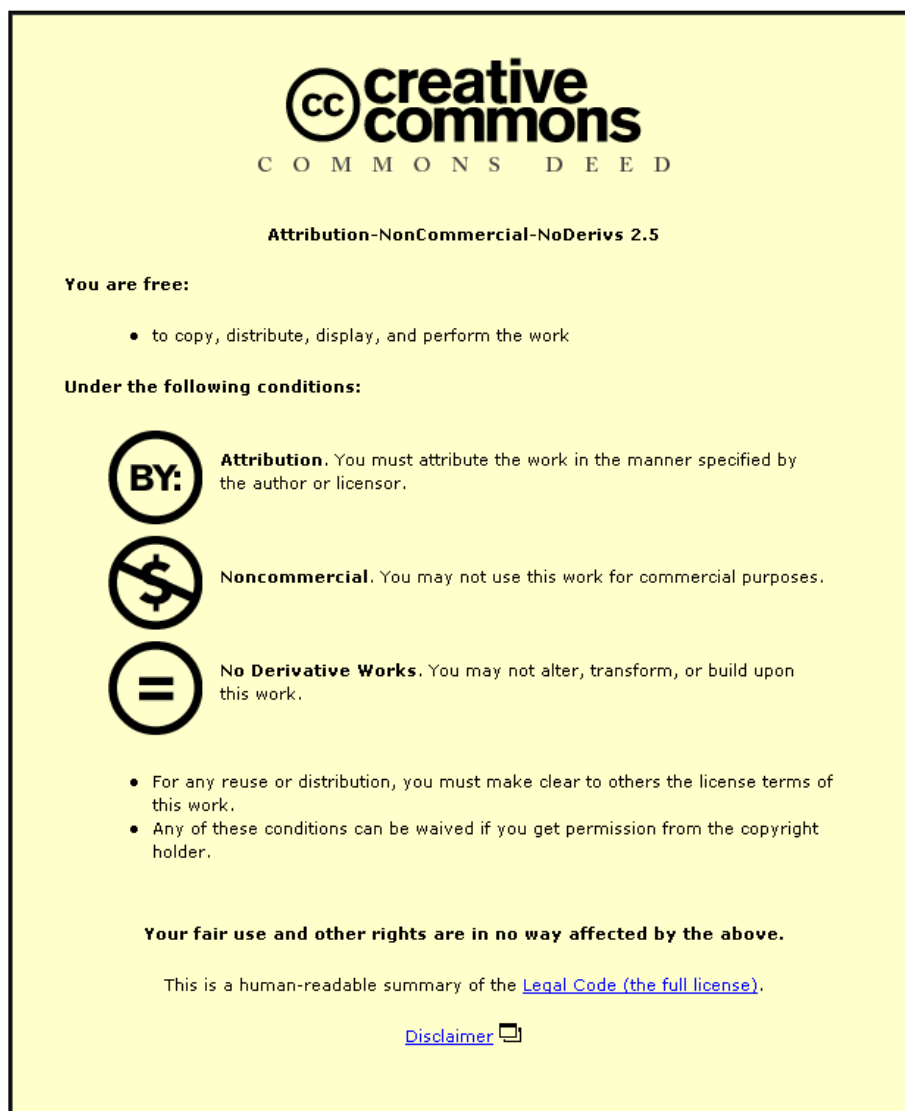




This item was submitted to Loughborough's Institutional Repository (<https://dspace.lboro.ac.uk/>) by the author and is made available under the following Creative Commons Licence conditions.



CC creative commons
COMMONS DEED

Attribution-NonCommercial-NoDerivs 2.5

You are free:

- to copy, distribute, display, and perform the work

Under the following conditions:

BY: **Attribution.** You must attribute the work in the manner specified by the author or licensor.


Noncommercial. You may not use this work for commercial purposes.

No Derivative Works. You may not alter, transform, or build upon this work.

- For any reuse or distribution, you must make clear to others the license terms of this work.
- Any of these conditions can be waived if you get permission from the copyright holder.

Your fair use and other rights are in no way affected by the above.

This is a human-readable summary of the [Legal Code \(the full license\)](#).

[Disclaimer](#) 

For the full text of this licence, please go to:
<http://creativecommons.org/licenses/by-nc-nd/2.5/>

Influence of haematocrit level on the kinetics of blood spreading on thin porous medium during dried blood spot sampling

Tzu Chieh Chao, Anna Trybala, Victor Starov, Diganta B. Das*

Department of Chemical Engineering, Loughborough University, Loughborough, LE11 3TU, UK

(*Corresponding author; Email: D.B.Das@lboro.ac.uk, Tel: 0044 1509 222509)

Abstract

Dried blood spotting (DBS) is a convenient blood collecting and sampling method which is widely applied in newborn screening and blood analysis. At the moment, the practice is to try to keep the blood within a marked circle in a thin porous filter paper. However, it is not always possible to predict exactly how the blood spot spreads inside the filter papers and it depends on many factors including the properties of the filter papers, blood properties and how the blood is deposited on the filter paper. In this paper, we aim to identify the relationships between the physical properties and the spreading behaviour of blood on a typical DBS filter paper (Whatman 903). Pig's blood was used to mimic the behaviour of human blood and investigate the spreading/imbibition processes of blood drops on the filter paper. Both top and side views were used to analyse the spreading/imbibition behaviour. The experimental data present the haematocrit effect on the spreading dynamics of blood for dried blood spot sampling. The results obtained prove that the spreading/imbibition time dependences of droplet height, droplet base radius and contact angle are universal function of dimensionless time.

Keywords: Dried blood spots (DBS), spreading dynamics, spreading experiment, dynamic contact angle, haematocrit level

1. Introduction

Dried blood spotting (DBS) is a convenient blood collecting and sampling method, which is widely applied in newborn screening and blood analysis. The ease of its use and a number of other benefits derived from advanced analytic technology have led to a rapid growth in the application of DBS in traditional screening methods (e.g., large scale neonatal screening) and others, e.g., preclinical test and, pharmacokinetic (PK), toxicokinetic (TK) and therapeutic drug monitoring (TDM) [1–8]. DBS provides many benefits compared to conventional whole blood collection or plasma sampling, such as low cost, ease of transport and storage, etc. [9]. These benefits are derived from the ability of DBS to collect, handle and store blood samples of micro-volumes from which qualitative and quantitative data can be obtained at a later date [1,2,10]. However, this method suffers from two main problems. First, the dispersion of blood analytes over filter paper is often found to be unequal which may cause inaccuracies in the clinical analysis of the collected blood [11]. Second, the current DBS methods may not be applied to

36 analyse certain analytes due to the small sampling volume and low recovery. The latter problem
37 has been benefitted from advanced analytical methods recently, such as liquid chromatography
38 tandem mass spectrometry (LC-MSMS) and high performance liquid chromatography-ultraviolet
39 (HPLC-UV) [1,2,6,10]. However, the issues mentioned above have always been the bottleneck of
40 practical application of DBS.

41
42 According to a number of review papers [3,6,7,10,12,13], most researches of DBS are focussed
43 on the metabolic disorder and clinical disease analyses, and studies on their fluid dynamical
44 behaviour (e.g., spreading kinetics of blood above and within the filter paper) are much less
45 visible [5–8]. At the moment, the practice is to try to keep the blood samples within a marked
46 circle in a thin porous filter paper. Recently, a significant amount of work has been spent trying to
47 find out how much the blood spot will spread (spreading behaviour) without trying to quantify the
48 kinetics of the wetting properties of the filter paper [2,9,11,12,14,15]. Also, a large amount of the
49 work seems to have been spent on trying to develop techniques for measuring concentrations of
50 solute/molecules from the collected blood sample on filter papers [2,7,10,12]. However, it is well
51 known that the spreading behaviour of blood droplets are not always possible to predict exactly
52 on the filter papers and it depends on many factors including the properties of the filter papers,
53 blood properties and the way how blood is deposited on the filter paper. Therefore, there is no
54 well-defined relationship between the theoretical and experimental parameters in the published
55 DBS literature and only few researches have considered the influence of spreading dynamics on
56 the DBS without quantifying these behaviour in detail [3,9,16]. In order to understand the
57 spreading processes accurately new model based on both theoretical and experimental methods
58 should be developed since the study of spreading behaviour of the blood drop over DBS filter
59 paper had not been developed before. In addressing these points, the spreading and imbibition
60 of blood droplets on thin porous media, namely, DBS filter paper is studied in this paper.

61
62 The kinetics of the spreading of other liquid drops over porous medium has been investigated in
63 previous studies [17–19]. According to the previous studies, the drop spreading over dry porous
64 layers is considered as two competitive processes: (i) the spreading of the drop over an
65 saturated porous surface and (ii) the imbibition of the liquid from the drop into the porous
66 substrate [20]. In this paper an axisymmetric experimental model of liquid drop spreading over a
67 thin porous layer is adopted as discussed in the next section. In the experiments, the dynamic
68 contact angles, droplet base radius and profile have been measured to characterize the
69 spreading process.

70

71 Although some of the above studies reported the spreading/imbibition of droplets of Newtonian
72 liquids on thin porous media, there is little or no study that has reported the spreading behaviour
73 of non-Newtonian fluids in general and, more specifically, blood in the context of DBS. Therefore,
74 the experimental investigation on blood spreading behaviour is essential. As mentioned earlier,
75 there are a number of parameters which affect the spreading behaviours of blood on filter papers.
76 Firstly, the physical properties of a filter paper, such as an average pore size and, thickness on
77 the layer affect the capacity and spreadability of blood on the filter paper. Considering the
78 consistency of the properties of DBS filter papers, the performance of filter paper was monitored
79 by the Newborn Screening Quality Assurance Program (NSQAP) at the Centers for Disease
80 Control and Prevention (CDC) (Atlanta, USA) to ensure that new filter paper are consistent with
81 established guideline [21]. Secondly, the properties of blood, including, blood rheology,
82 haematocrit level (i.e., the volume fraction of red blood cells in blood) and drop volume affect the
83 performance of blood spreading/imbibition.

84

85 It is well known that the blood rheology is affected by the haematocrit level [22,23]. Further, the
86 significance of haematocrit level to dried blood sampling has been discussed earlier [9,11,24–26].
87 For example, it was reported that the levels of most amino acids and free carnitine were higher in
88 the blood drop periphery than in the central spot with lower haematocrit level [11]. Denniff and
89 Spooner [9] reported that a bias was observed in the concentration of two analytes at different
90 haematocrit levels and the area of DBS samples decreased linearly with increasing haematocrit
91 levels. [9]. O'Mara et al. [24] reported that a significant bias (>15%) existed due to the
92 haematocrit effects and unequal distribution across the spot. This shows that the influence of
93 haematocrit levels on the concentration of analytes would be case-dependent, i.e., analyte
94 concentration could vary in different cases of the DBS samples, which could be caused by
95 unequal distribution of analytes in plasma, red blood cells or both [25]. In order to utilize DBS
96 accurately in clinical analyses, the haematocrit effects should be investigated as a method
97 development and validation for individual analyte. Generally speaking, it is expected that the
98 influence of the spreading kinetics of blood droplet at different haematocrit level to the DBS
99 sampling is much more consistent although the spreading kinetics is determined by the rheology
100 of blood, which again depends on haematocrit level. Nevertheless, the spreading kinetics of
101 blood at different haematocrit levels should be investigated further to provide a better
102 consideration of the influence of haematocrit level differences to the whole DBS sampling and
103 analysis process.

104

105 In addressing the above issues, a series of experiments is presented in this paper to investigate
106 the spreading/imbibition behaviour of blood droplets with different haematocrit levels on DBS

107 filter papers. The experiments are aimed at recording blood drop spreading/imbibition behaviour
108 over the filter paper using a high speed camera and analysing the spreading droplet radius,
109 volume, wetted area inside the filter paper and contact angle by an image analytic software
110 [17,19,27]. The whole process requires special conditions in which they are carried out as the
111 spreading/imbibition experiment data may be influenced by environmental factors such as, gas
112 flow, vibration and horizontal level. Therefore, in our experiment, a special hermetically isolated
113 chamber has been designed and installed on a vibration-protected table to eliminate the
114 environmental effects during the drop spreading experiments. In order to quantify the blood
115 spreading process, we observe the wetted region on the surface of filter paper (top view) as well
116 as the droplet spreading and absorption behaviour (side view). The wetting region on the surface
117 of the filter paper is known as the dried blood spots sample area. According to Starov et al. [19],
118 the spreading behaviour of liquid droplet over porous layer (filter paper in our case) could be
119 considered as overlapping of two different processes: one is the spreading of blood over the filter
120 paper; another is the capillary motion inside the matrix of the filter paper. In consistent with this
121 study, the time evolution of the radius of the wetting region, the drop base, the drop volume and
122 the contact angle were monitored in our experiments.

123

124 We use pig's blood with different haematocrit levels to simulate the behaviour of human blood,
125 and observe the spreading process of the liquid drops on DBS filter paper to analyse its
126 spreading behaviour. The selection of the animal blood as a simulant for human blood in our
127 experiments is based on the similarity of its rheological properties to those of human blood,
128 namely, the blood viscosity, plasma viscosity, erythrocyte aggregation and others [28]. The easy
129 availability of pig's blood from nearby abattoir and the ethical policy on minimum or no use of
130 human blood for laboratory experiments are other considerations in our design of experiments.
131 Accordingly, pig's blood is considered as the most suitable blood simulant in our experiments.
132 The blood rheology was obtained via in-house laboratory experiments and used to identify the
133 difference of spreading behaviour between blood samples with different haematocrit levels. The
134 spreading behaviours of blood plasma and water on the same filter paper are also analysed as
135 reference liquid and used to characterise the effects of the presence of red blood cells (RBCs) to
136 the spreading behaviour of pure liquid.

137

138 **2. Materials and Experimental Methods**

139 **2.1. Blood**

140 Pig's blood was collected in EDTA anti-coagulated tubes (International Scientific Supplies Ltd.
141 Bradford, UK) from a local butcher. 0.9% sterile saline solution (OXOID Ltd., Hampshire, UK)

142 was used to wash red blood cells after centrifugation. Blood was stored at 4°C and all blood
143 samples were used within 4 hours after collection.

144 **2.1.1 Preparation of different haematocrit levels of blood**

145 Blood of different haematocrit levels was prepared according to the procedures presented by
146 Baskurt et al. [23]. The blood samples with different haematocrit levels were centrifuged by a
147 Heraeus Labofuge 400R centrifuge (Thermo scientific, UK) at a constant rotating speed (~1400 g)
148 for 10 minutes to separate the red blood cells (RBC) and plasma without damaging the RBC in
149 the blood. After the separation, the plasma was kept for re-suspension later and the cells were
150 washed by the sterile saline solution three times to remove buffy coat layer, i.e., a thin layer that
151 is generated between plasma and RBC after centrifugation, which also contains most of the
152 white blood cells and platelets. The washed cells were then re-suspended in plasma at the
153 required haematocrit levels, namely, 0%, 30%, 50% and 70%.

154
155 After the preparation of blood samples, the haematocrit level and cell density were measured for
156 every sample to make sure consistency in the quality of the samples.

157

158 **2.1.2 Measurements of blood rheology**

159 As described in section 2.1.1, blood samples with different haematocrit levels (0%, 30%, 50%,
160 and 70%) were prepared from single source and slowly vibrated to a well-mixed condition at
161 room temperature before testing. The blood rheology measurements have been made using the
162 rheometer with plane geometry (4 cm diameter, stainless steel) and 250 µm gap. The
163 temperature was kept constant using Peltier plate at 25°C. The viscosity measurements have
164 been made in shear rate range 0.2 to 100 s⁻¹. Also the blood density was measured using a
165 pycnometer at 25°C.

166 **2.2. Filter paper characteristic**

167 Whatman 903 blood spot cards were supplied by Whatman (GE Healthcare, Maidstone, UK).
168 Riechert-Jung MEF3 inverted microscope accompanied with the digital image acquisition via
169 QCapture software are used to estimate the filter paper thickness. Carl Zeiss (Leo Cambridge)
170 Stereoscan 360 Scanning electron microscopy (SEM) was applied to provide the scanning
171 electron micrographs which are then used to determine the thickness, the surface porosity and
172 the pore size distribution. All the experimental results for filter paper thickness are calculated
173 from SEM and inverted optical microscope images via Image J software.

174 **2.3. Spreading experiment**

175 The spreading of blood with different haematocrit levels was observed from both side and top.
176 Each spreading data were determined from ten replicate blood spot, each derived from 10 µl

177 blood samples, at 0%, 30%, 50% and 70% haematocrit levels on DBS filter paper. Each droplet
178 sample was produced via a 10.0 ± 0.5 μl syringe in our experiments. Furthermore, the initial
179 volumes of the blood droplets were calculated and checked from images recorded by high speed
180 camera for all the spreading experiments. Hence, the experiments conducted in this work ensure
181 repeatability of initial droplet volume within a range of around 10.0 ± 0.5 μl . All the video images
182 were taken from printed side of DBS filter paper with a constant working distance and focal
183 length.

184

185 Cameras that have been used in spreading experiment are AVT Pike F-032 high performance
186 camera (Allied Vision Technologies, UK) for the top views recording and i-SPEED LT high speed
187 video camera (Olympus, UK) for the side views. The optical objective used in side view
188 experiment for small drop spreading is IF-3 standard (INFINITY PHOTO-OPTICAL GmbH,
189 Germany). AR1000-N Rheometer (TA instrument, USA) was used to determine the viscosity of
190 blood.

191

192 The experimental set up of spreading experiment is shown in Figure 1, which is based on the
193 experiment setup used earlier for the droplet spreading/imbibition experiments with Newtonian
194 liquids [20]. A filter paper substrate is placed in a closed chamber with a fixed temperature and
195 humidity. The chamber was equipped with optical glass windows for observation of both the
196 shape and the size of the spreading drops; a side view and top view were monitored. The light
197 source was installed at the bottom and the other side of chamber where the light can come from
198 the opposite site of the CCD camera. The chamber and all optical equipment were mounted on
199 an optical bench. The optical bench was installed on a vibration-protected table.

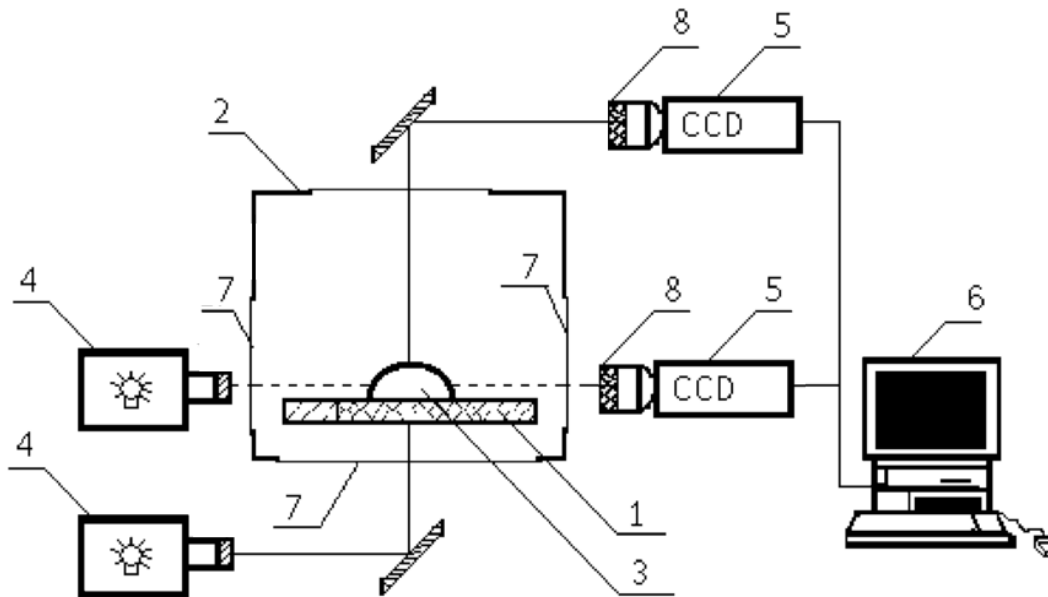
200

201 The experiments were processed in the following order for obtaining both side and top views of
202 blood spreading:

203

- 204 a) The porous substrate under investigation (filter paper) was placed in the chamber.
- 205 b) Optical equipment was adjusted to focus on the sample depositing spot and the spreading
206 process area, where the equipment include: CCD camera lenses, light source based on
207 working distance.
- 208 c) A droplet of investigated sample (blood) was placed on the substrate by syringe and the
209 whole process was recorded by CCD cameras.
- 210 d) Calibration of known distance in each image was done with identified micro-scale.

211 e) The image was analysed to obtain experimental data via image processing software (ImageJ
 212 and Vision builder (National Instrument, UK)) which are able to record specific parameters
 213 such as droplet radius, height and wetting region and quantify the obtained data.
 214



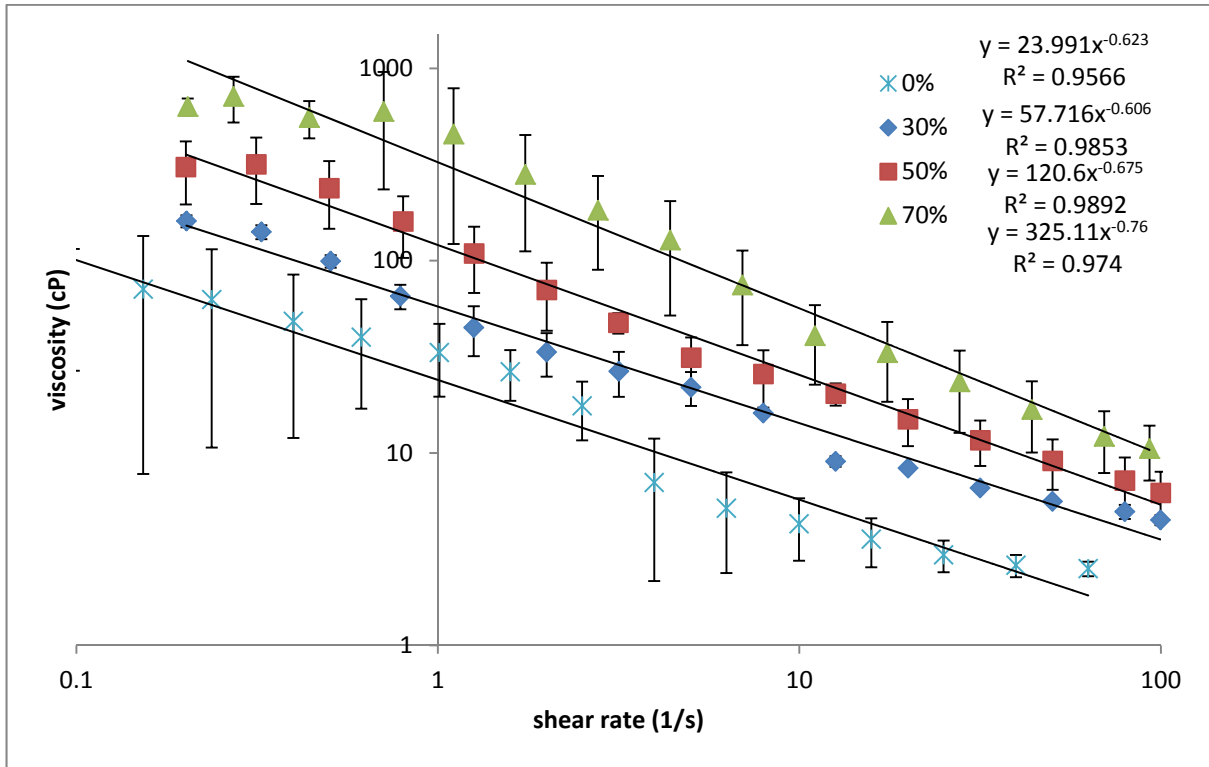
215
 216 Figure 1. Sketch of the experimental set-up: 1, porous substrate; 2, hermetically closed,
 217 thermostated chamber, 3, liquid drop; 4, light sources; 5, CCD cameras; 6, PC; 7, optical
 218 windows; 8, optical objectives.

219 **3. Results and Discussions**

220 **3.1 Rheology of blood used in spreading experiments**

221 The rheology of blood is an important parameter in the spreading dynamics over porous medium.
 222 The influence of haematocrit level of blood viscosity was investigated by measuring the blood
 223 viscosity at different haematocrit levels. In particular they were measured so as to characterise
 224 the blood samples used in this study. The viscosity values were measured at 25°C, which are
 225 shown in Figure 2. As expected, the shear thinning character of the blood was found. At high
 226 shear rate, the value of viscosity of blood decreases to a constant low number of around 4-15 cP.
 227 However, at low shear rate the blood viscosity varies from 1000cP to 400cP which may be
 228 caused by the unequal aggregation of RBCs and the formation of suspended particles inside the
 229 blood [23]. Figure 2 shows that the viscosity of blood is higher as the haematocrit level increases.
 230 The experimental data presented in the figure are in a good agreement with other reference data
 231 [28,29]. The data are also in good agreement with Thiriet's study [30] in which the author shows
 232 that the values of blood viscosity at constant temperature can be approximated by following
 233 power law equation:

234 $\mu = k\dot{\gamma}^{n-1}$ (1)
 235 where k and n are consistency factor and flow behaviour index, μ is blood viscosity and $\dot{\gamma}$ is the
 236 shear rate. Equation (1) can be rewritten as $\ln \mu = \ln k - n \ln \dot{\gamma}$ and we use Table 1 to fit the
 237 parameters k and n.
 238



239
 240 Figure 2. The dependency of blood viscosity at 0%, 30%, 50% and 70% haematocrit levels on
 241 shear rate from 0.5 s^{-1} to 100.0 s^{-1}
 242

243 Table 1. Fitted values of k and n according to equation (1)

Haematocrit levels in blood	k	n
0%	23.99	0.368
30%	57.72	0.394
50%	120.60	0.325
70%	325.11	0.240

244
 245 As shown in Table 1, the values of n are almost constant and it is slightly higher with higher
 246 haematocrit level. However, the values of k vary significantly with different haematocrit levels.
 247 These show that the viscosity values of blood follow a universal function of shear rate, where the
 248 values increase with increasing haematocrit levels.
 249

250 The average densities of the blood sample used in this study are shown in Table 2. The results
251 show that the density of blood sample with higher haematocrit level is higher than blood samples
252 with lesser haematocrit level.

253

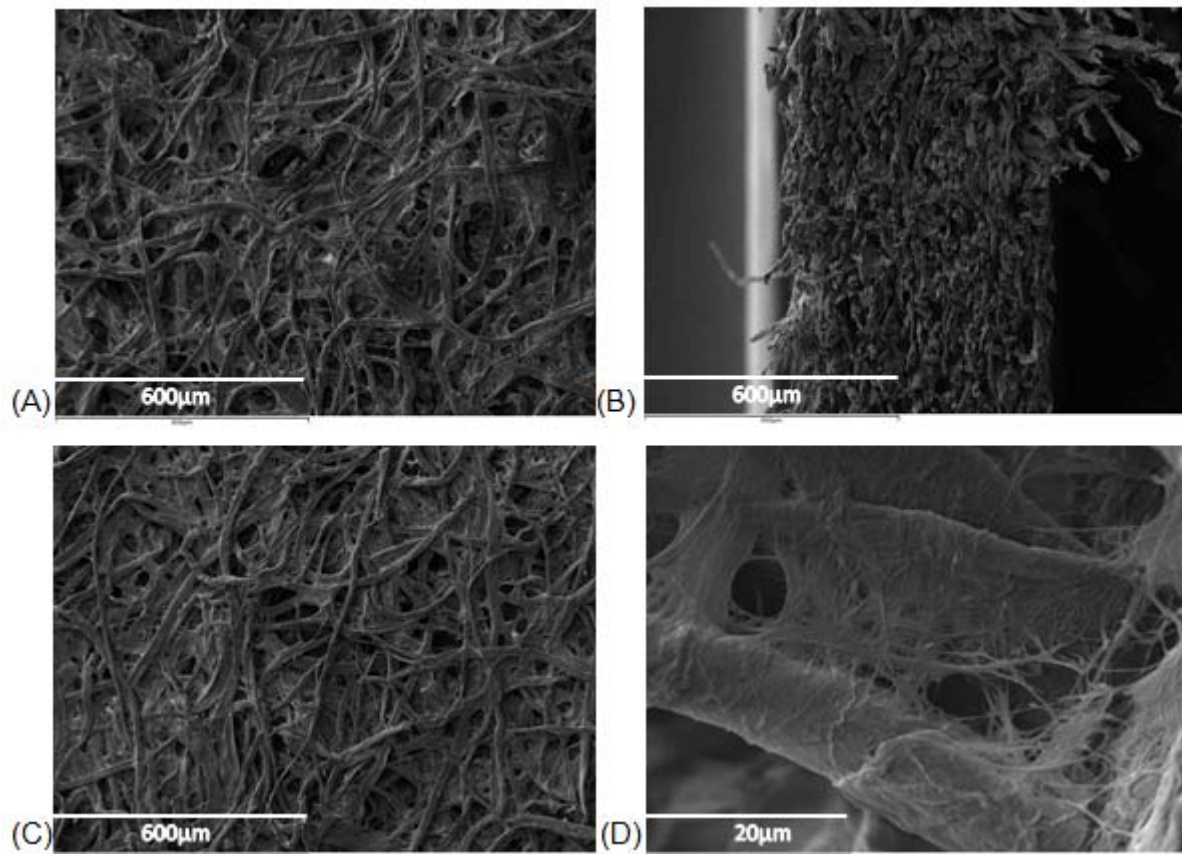
254 Table 2. The average density of plasma and blood at 30%, 50% and 70% haematocrit levels at
255 25°C (data were calculated based on 3 samples)

Fluid Sample	Average Density (kg/m ³)
Plasma (0% haematocrit level in pig's blood)	1030.52±0.13
30% haematocrit level in pig's blood	1043.18±1.32
50% haematocrit level in pig's blood	1049.75±1.75
70% haematocrit level in pig's blood	1058.71±2.21

256

257 3.2 Characteristics of filter paper

258 The spreading/imbibition behaviour of blood droplet over porous filter paper depends on the
259 physical properties of filter paper used: the thickness, fibre matrix composition, permeability,
260 porosity and pores size distribution. We used two microscopes to observe the surface
261 heterogeneity and measure the thickness of filter paper, in order to analyse these physical
262 parameters under different scale levels (Figure 3). In Figure 3, the images have clearly shown
263 that the pores inside the filter paper are created from both the space between the fibre structure
264 and the micro pores of fibres itself. The thickness of filter paper was also measured from the
265 cross sectional images of the filter paper which were taken by an inverted microscopy. The
266 average thickness data were obtained and calculated from 5 random cross sections per image
267 via an image processing software, namely, QCapture (Qimaging, Canada). The image taken by
268 polarized optical microscopy shows that the average thickness of the filter paper is around $\Delta=500$
269 $\pm 50 \mu\text{m}$, which is a good agreement with data calculated from 10 different samples using direct
270 measurement of the thickness by a micrometre. The intrinsic permeability of the completely wet
271 filter paper was measured using a porometer (Porous Materials Inc., US) which was found to be
272 $0.56\pm 0.025 \mu\text{m}^2$. The basic principle of porometer test is that it forces a non-reactive gas (air in
273 this study) flow through the porous sample with increasing pressure steps to push out the wetting
274 liquid inside porous material. This provides a relationship between the flow rate and pressure
275 difference which is then used to determine the permeability (i.e., Darcy law)[31]



276

277

278

Figure 3. The micrographs of filter paper at (A) top, (B) side and (C) bottom sides under 600 μm scale and (D) 20 μm scale from scanning electron microscopy (SEM)

279

3.3 Kinetics of blood droplet spreading

280

281

282

283

284

285

286

287

The images captured from top and side views were analysed for all spreading/imbibition experiments. The drop spreading/imbibition were assumed to be symmetric over the whole duration of the process and the contact area of the drop on the surface of the porous filter paper was assumed to be circular. These assumptions were in a good agreement with our experimental observations of blood spreading/imbibition processes. Spherical form of the spreading drop was used to calculate the volume of the drop that lies over the substrate as a function of time. The schematic is shown in Figure 4.

288

289

290

291

292

293

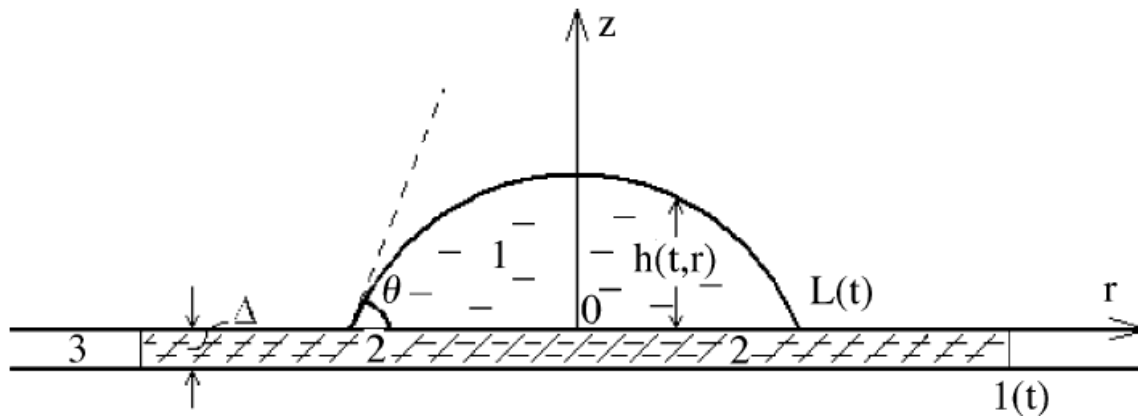
294

The wetted region inside the filter paper, $l(t)$, was obtained using top view video photographs at 60 fps (Figure 5). These image sequences were processed using ImageJ software to obtain the area $A(t)$ and perimeter $P(t)$ of each spot. A distance was defined on the image of an identified micro-scale using the software calibration; this was then used to measure the area of the DBS samples after transforming the image into black and white. The hydraulic radius of wetting region $l(t)$ was then calculated as follows:

295 $l(t) = 2A(t)/P(t)$

(2)

296



297

298

299

300

301

302

303

Figure 4. Cross-section of the axis-symmetric spreading drop over initially dry filter paper with thickness Δ . 1 -liquid drop; 2 - wetted region inside the porous substrate; 3 - dry region inside the porous substrate. $L(t)$ - radius of the drop base; $l(t)$ - radius of the wetted area inside the porous substrate; Δ -thickness of porous substrate, r, z co-ordinate system; $h(t, r)$ -profile of the spreading drop; θ -contact angle.

304

305

306

307

308

309

310

311

312

313

The time dependency of the radii of wetting regions, $l(t)$, for pure water and blood at 0%, 30%, 50% and 70% haematocrit levels on Whatman 903 filter paper at 25°C are shown in Figure 6. Figure 6 shows that the spreading process inside the filter paper can be divided into two stages in the case of pure water and plasma (0% haematocrit blood). The first stage of the penetration of fluid inside the filter paper is caused by the imbibition of the blood from the droplet transport into big pores. As a result the wetted region increased very fast. After the imbibition of droplet was completed, the second stage involves the penetration of fluid inside the filter paper, which is caused by the fluid penetration from larger pores into smaller pores, where the spreading kinetic is much slower.

314

315

316

317

318

319

320

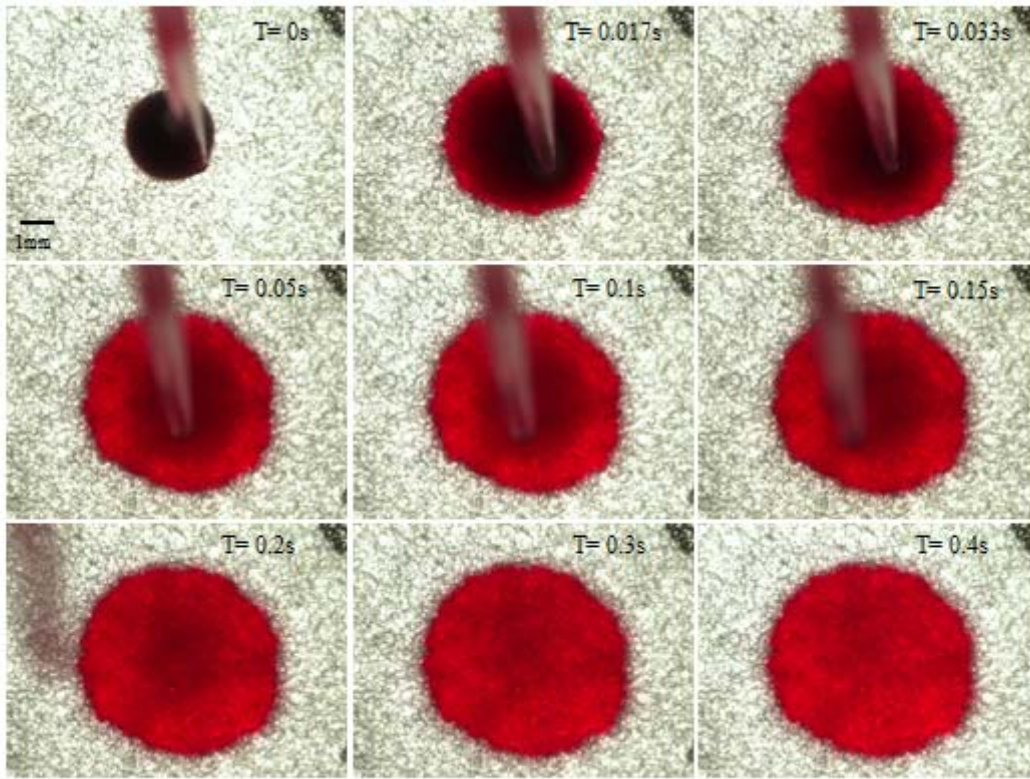
321

322

323

According to Figure 6 there is a significant difference in the radius of wetted region in the case of (1) the water (Newtonian liquid) and (2) plasma and blood samples (shear thinning liquids). First of all, the radius of wetting region of water is much bigger than in the case of plasma and blood samples. In the case of plasma/blood samples, the radius of the wetted region reached its maximum value within around 0.4 second and stopped expanding further. On the other hand, the water drops spread continuously for a prolonged period of time after the droplet spreading was completed. Water continued to spread inside the filter paper after the droplet on the filter paper already disappeared. However, all the plasma/blood samples stopped penetrating around the same time when the droplet was completely imbibed into filter paper. These results indicate that the presence of RBCs change considerably the spreading behaviour of blood inside the filter

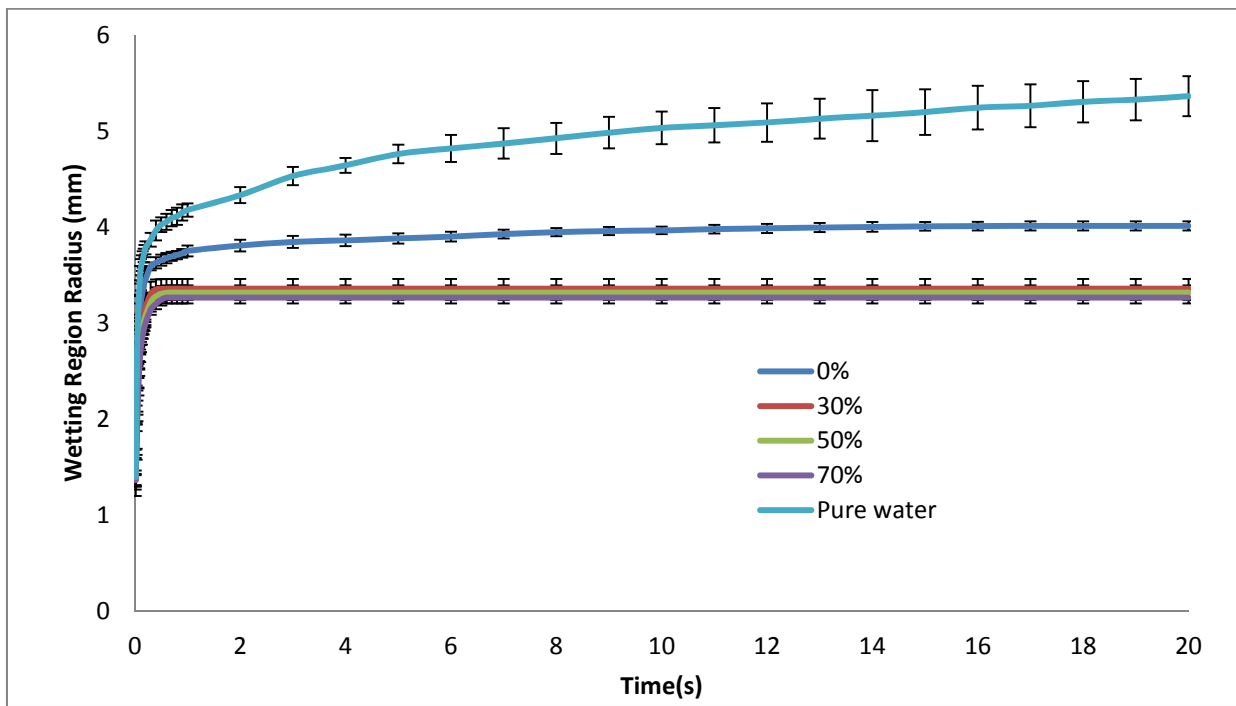
324 paper, where the blood samples remained inside a constant small region while water continues
325 to penetrate inside the filter paper.



326
327 Figure 5. Top views of 30% haematocrit blood spreading on filter paper. Each image was
328 captured at 60 fps from the time the first image was taken

329
330 According to Starov et al. [19], the main mechanisms of spreading behaviour of a liquid drop
331 inside and over the porous substrate are viscosity and capillary forces. The capillary forces do
332 not change a lot with the haematocrit difference as the fluid properties are almost same in the
333 interfacial. Therefore, the viscosity difference between plasma and blood should be the major
334 mechanism to be responsible for the spreading behaviour inside the porous fibre. According to
335 our measurements (Figure 2) both plasma and blood show a shear thinning behaviour. After the
336 blood is imbibed into filter paper, the shear rate of blood decreased and the latter results in the
337 increasing of blood viscosity, which further decrease the spreading kinetic inside the filter paper
338 and eventually prevent the further penetration of blood. In physical terms the latter means that
339 the red blood cells block the micro-pores in the filter paper and as a result the plasma cannot
340 penetrate from the large pores into smaller pores.

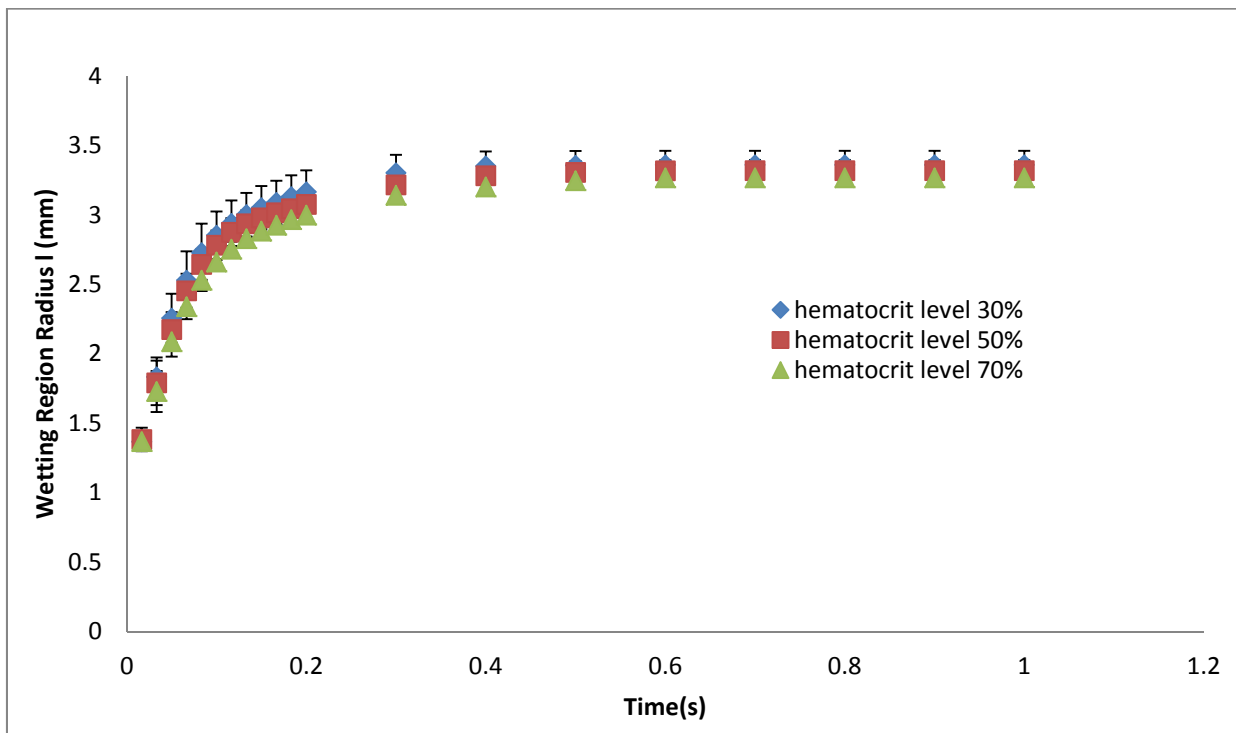
341



342

343 Figure 6. Time evolution of radius of wetted region, $l(t)$, inside the filter paper: plasma, pure water
 344 and 30%, 50%, 70% haematocrit levels in blood

345



346

347 Figure 7. The spreading radii of wetting regions of blood at different haematocrit levels

348

349 In Figure 7, a magnification of the data presented in Figure 6 is given on the time dependency of
 350 the wetted region inside the filter paper for blood at different haematocrit levels. Figure 7 shows

351 that the maximum radius of the wetted area slightly decreases with higher haematocrit level: the
352 maximum radius difference between 30% and 70% haematocrit blood are around 3%. This result
353 has been noticed earlier [9,11]. Figure 7 also shows that the higher haematocrit level is the
354 slower the spreading is.

355

356 The time variation of the drop base radius, $L(t)$, and the height of drop of the drop, $h(t, r)$, were
357 obtained using side view and high speed video camera (600 fps) (Figure 8). The images were
358 processed using vision builder software, where the volume of the spherical cap and the contact
359 angle formed by the fluid with substrate was calculated as follows[20]:

360

$$361 \quad r_c = \frac{(L(t)^2 + h_c^2)}{2h_c} \quad (3)$$

$$362 \quad \theta = 90 - \frac{180}{\pi} \sin^{-1} \left(\frac{r_c - h_c}{r_c} \right), \quad (4)$$

363

364 where h_c is the height of the drop at central point, r_c is the contact radius, and θ is the contact
365 angle.

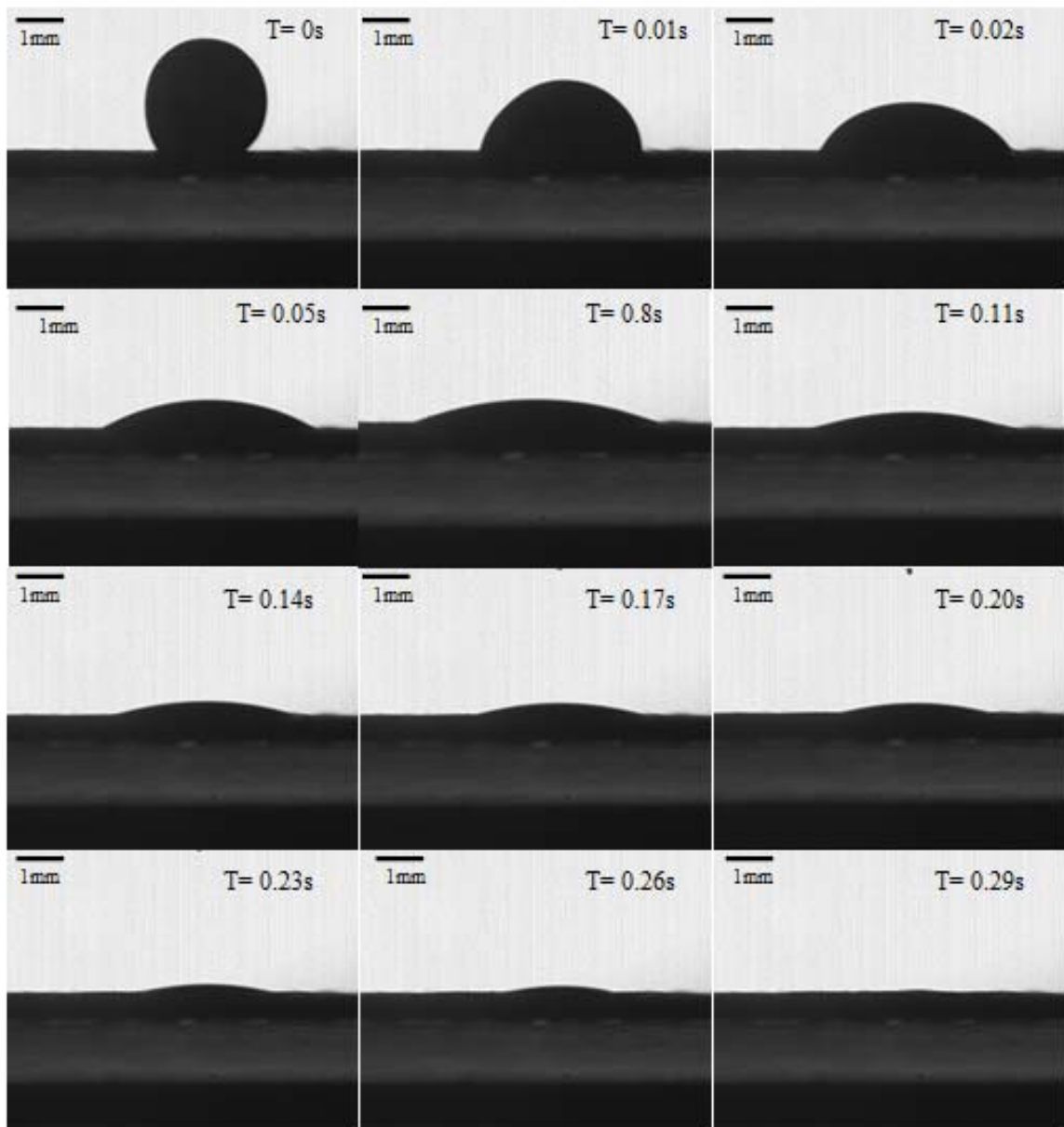
366

367 According to our experimental observation the radius of drop base initially increases to its
368 maximum value and then slowly decreases till complete imbibition of blood drops. The most
369 notable differences between the samples with different haematocrit levels are the spreading
370 kinetic as shown in Figure 9. The time of completely imbibition is around 0.2 second for plasma.
371 However, the imbibition times for blood samples at 30%, 50% and 70% are slower and are
372 around 0.3s, 0.45s and 0.6s. This result clearly suggests that the spreading kinetic decreases as
373 the haematocrit level increases or the same as the viscosity increases.

374

375 In order to further discuss the spreading dynamics of droplet spreading over porous media, the
376 spreading radius, contact angel and droplet height have been suggested to use the
377 dimensionless unit as follows [19]: $L(t)/L_m$, $\theta(t)/\theta_m$, $h(t)/h_m$ on dimensionless time: t/t^* , where
378 L_m is the maximum radius of the droplet base; θ_m and $h_m(t)$ are the contact angle and droplet
379 height when the spreading radius reaches the maximum value; t^* is the time of complete
380 imbibition of the blood droplet. All the relevant data are shown in Table 3.

381



382

383

384 Figure 8. Side views of 30% blood spreading over Whatman 903 filter paper. Each image is

385

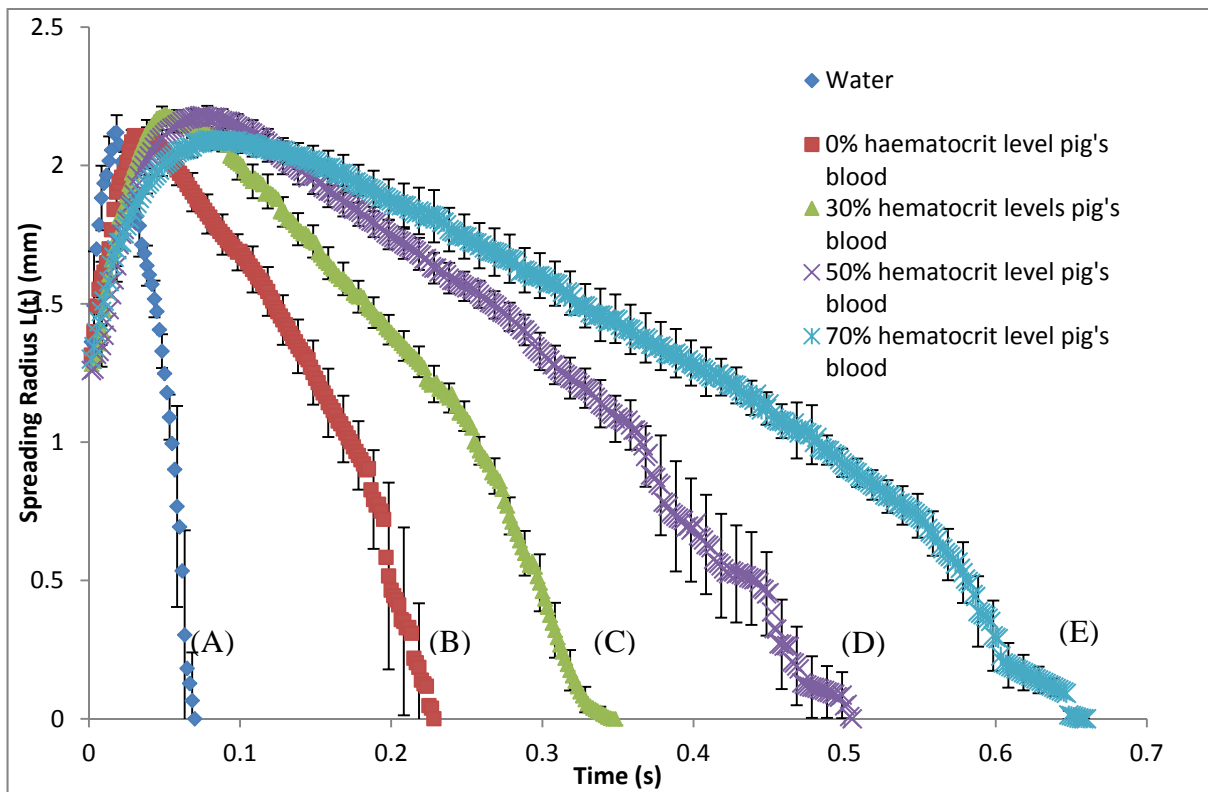
0.01 s and for following sequence is 0.03s

386

387 Table 3. Time of complete imbibition, maximum spreading radius of droplet base, droplet height
 388 at maximum spreading and contact angle at maximum spreading for investigated blood samples.

	t^* (s) Time of complete imbibition	L_m (mm) Maximum spreading radius of droplet base	h_m (mm) Droplet height at maximum spreading	θ_m (degree) Contact angle at maximum spreading
Water	0.072	2.12	0.51	29.62
0% haematocrit level	0.230	2.11	0.66	34.44
30% haematocrit level	0.351	2.18	0.65	32.80
50% haematocrit level	0.508	2.18	0.62	30.94
70% haematocrit level	0.663	2.09	0.62	33.48

389



390

391 Figure 9. Radii of the drop bases as function time: (A) 10 μ l water, (B) 10 μ l 0% blood (C) 10 μ l
 392 30% blood (D) 10 μ l 50% blood (E) 10 μ l 70% blood on Whatman 903 filter paper.

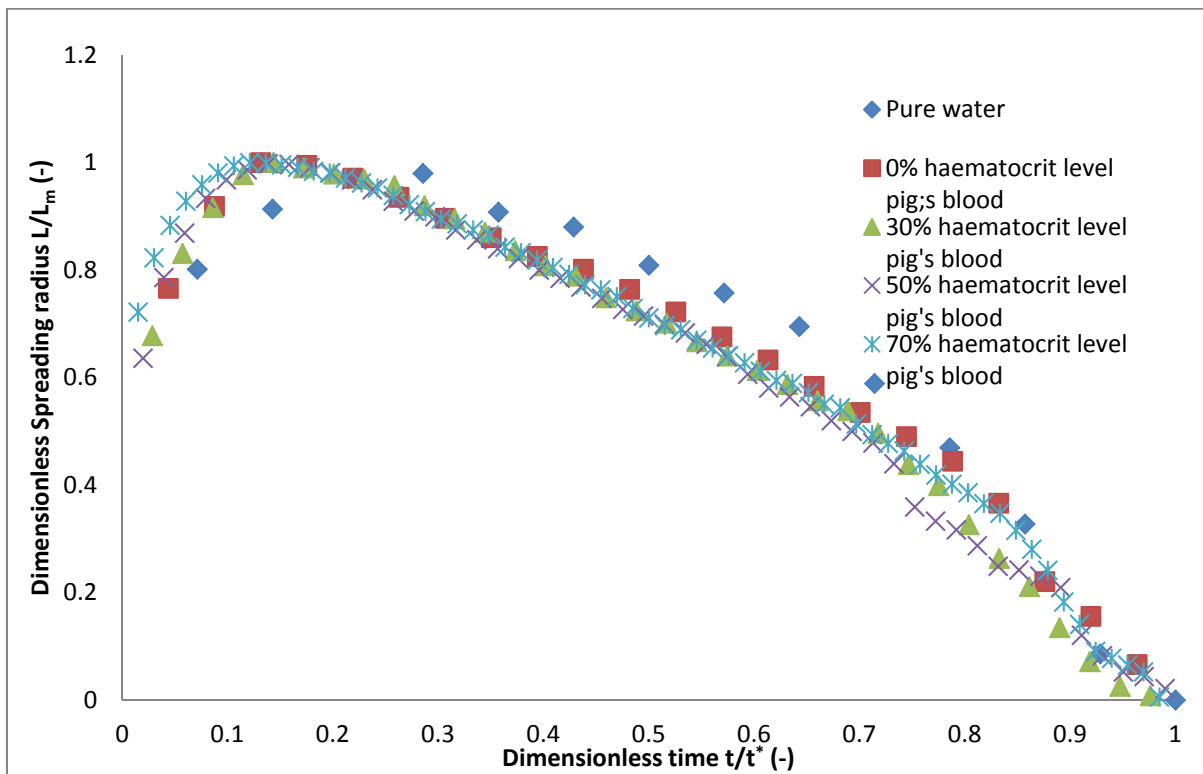
393

394 In Figures 10 and 11 the spreading behaviours of pure water and blood with different haematocrit
 395 levels in dimensionless units. The dimensionless time scales of blood at different haematocrit
 396 levels required to reach the maximum radius of the drop base and completely imbibition are
 397 relatively similar compared to water. In reference to the dimensionless time in Figure 10, the

398 spreading behaviour of water shows that water has less retention time above the filter paper as
399 compared to that of blood droplets. This indicates that water (a Newtonian liquid) may penetrate
400 easily into the filter paper in comparison to that of the blood samples.

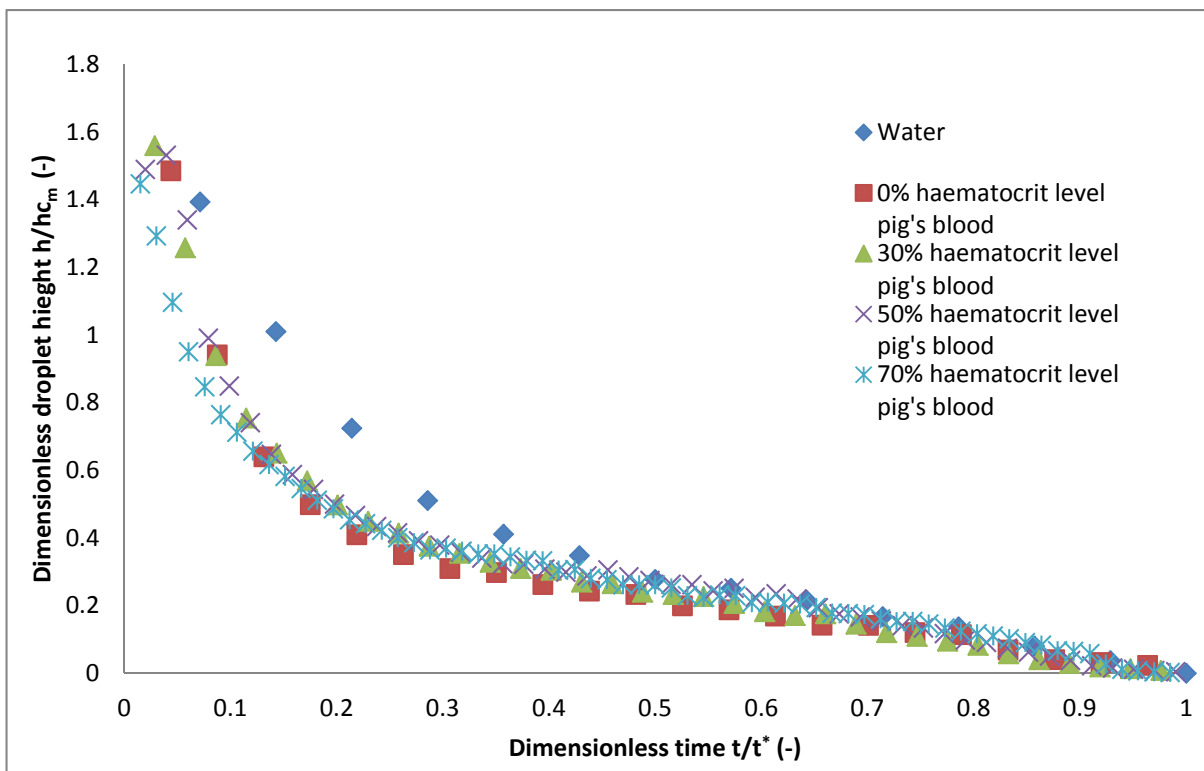
401
402 Figures 10-12 demonstrate that the time evolution of droplet base, height and contact angle in
403 the case of Newtonian liquid (water) is different from the corresponding dependences of non-
404 Newtonian liquids: blood droplet at different haematocrit levels. However, the qualitative
405 behaviour of all dependences in the case of Newtonian and non-Newtonian liquids remains
406 similar. The time evolution of spreading radius of blood on time can be divided into two stages in
407 the case spreading/imbibition process of blood droplet over filter paper as in the case of
408 Newtonian liquids [19]. The two competing processes determine the whole spreading process:
409 the spreading of blood droplet, which results in an increase of the radius of the droplet base and
410 the imbibition of blood from droplet into the filter paper, which results in a shrinkage of the droplet
411 base. At the beginning, the base radius of droplet expanded to the maximum value. When the
412 droplet base radius started to decrease and the contact angle remained constant till complete
413 disappearance of the droplet. According to this two stage theory, the spreading behaviour of
414 blood and plasma show a similar behaviour. Two stages of the process prove that the spreading
415 of plasma and blood at all haematocrit levels are governed by a complete wetting of the filter
416 paper and in this case the spreading processes proceed in two stages [20]. Otherwise three
417 stages of the spreading/imbibition would exist [32].

418



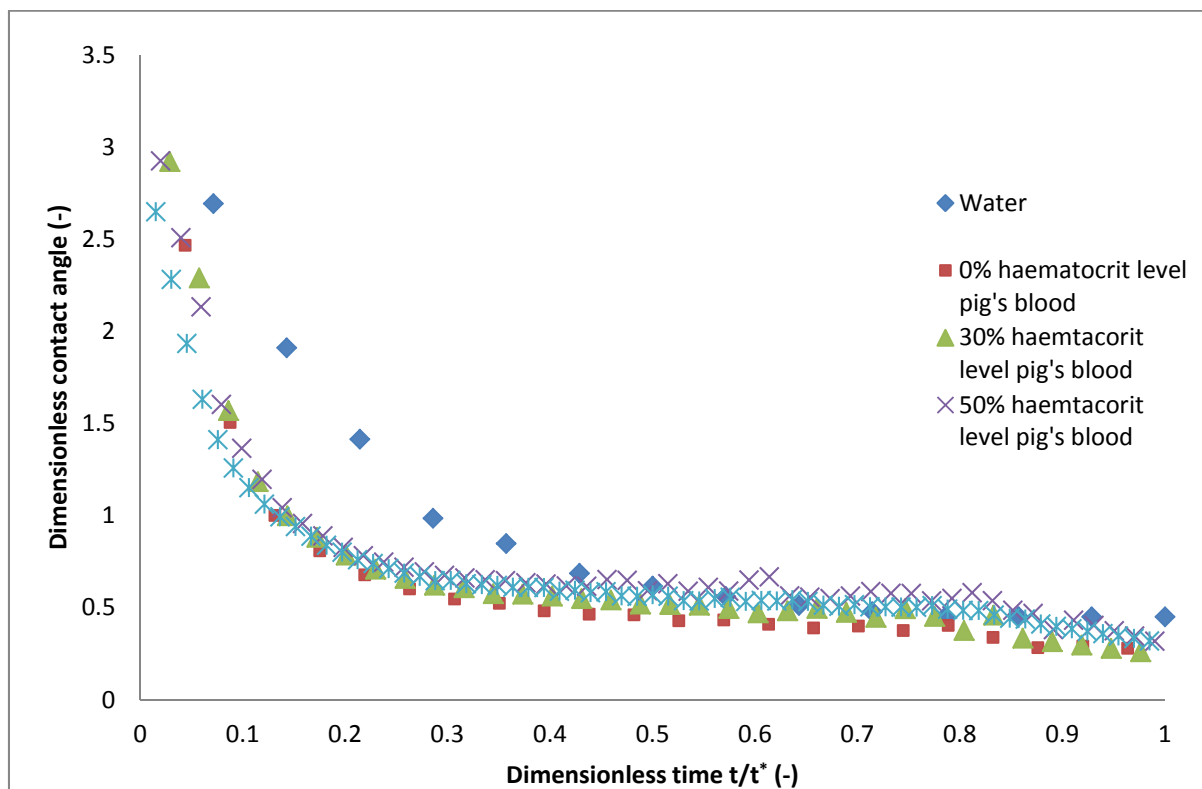
419
420
421

Figure 10. Dimensionless radii of the drop base as function of dimensionless time for water and blood samples at 0%, 30%, 50% and 70% haematocrit levels



422
423
424

Figure 11. Dimensionless droplet heights of water, blood 0%, 30%, 50% and 70% haematocrit blood as function of dimensionless time



425
 426 Figure 12. Dimensionless dynamic contact angles of water, blood plasma, 30%, 50% and 70%
 427 haematocrit blood as function of dimensionless time
 428

429 **Conclusion**

430 In this paper we have discussed the influence of different haematocrit levels of blood on the
 431 spreading/imbibition dynamics of DBS sampling on filter paper. For the droplet spreading over
 432 the filter paper, the size and spreading kinetic of blood samples on Whatman 903 filter paper has
 433 been demonstrated to decrease proportionally with the increase of haematocrit level in the blood.
 434 There is a significant decrease of wetting region as the presence of RBCs in blood plasma which
 435 indicates that the presence of RBCs in plasma-like solution considerably change the
 436 spreading/imbibition kinetics through porous fibre due to the shear-thinning behaviour of blood.
 437 The experimental data present the haematocrit effect on the spreading/imbibition dynamics of
 438 DBS sampling. The results suggest that all the spreading/imbibition dependences such as
 439 droplet height, droplet base radius and contact angle can be presented as universal functions of
 440 dimension less time. This behaviour of blood spreading allows us to control and calculate several
 441 spreading parameters of DBS sampling, such as, wetting region, retention volume, imbibition
 442 volume, liquid retention time above filter paper, etc. The development of a theoretical model
 443 based on the experimental data of spreading behaviour for determining the distribution of specific
 444 analytes is being considered and will be presented in our future work.

445 **Bibliography**

- 446 1. Edelbroek, P. M.; Van der Heijden, J.; Stolk, L. M. L. Dried blood spot methods in therapeutic
447 drug monitoring: methods, assays, and pitfalls. *Therapeutic drug monitoring* **2009**, *31*, 327–36.
- 448 2. Li, W.; Tse, F. L. S. Dried blood spot sampling in combination with LC-MS/MS for quantitative
449 analysis of small molecules. *Biomedical chromatography : BMC* **2010**, *24*, 49–65.
- 450 3. Spooner, N.; Lad, R.; Barfield, M. Dried blood spots as a sample collection technique for the
451 determination of pharmacokinetics in clinical studies: considerations for the validation of a
452 quantitative bioanalytical method. *Analytical chemistry* **2009**, *81*, 1557–63.
- 453 4. Chaillet, P.; Zachariah, R.; Harries, K.; Rusanganwa, E.; Harries, a D. Dried blood spots are a
454 useful tool for quality assurance of rapid HIV testing in Kigali, Rwanda. *Transactions of the Royal
455 Society of Tropical Medicine and Hygiene* **2009**, *103*, 634–7.
- 456 5. Déglon, J.; Thomas, A.; Mangin, P.; Staub, C. Direct analysis of dried blood spots coupled with
457 mass spectrometry: concepts and biomedical applications. *Analytical and bioanalytical chemistry*
458 **2012**, *402*, 2485–98.
- 459 6. Barfield, M.; Spooner, N.; Lad, R.; Parry, S.; Fowles, S. Application of dried blood spots
460 combined with HPLC-MS/MS for the quantification of acetaminophen in toxicokinetic studies.
461 *Journal of Chromatography B* **2008**, *870*, 32–37.
- 462 7. Demirev, P. a Dried blood spots: analysis and applications. *Analytical chemistry* **2013**, *85*,
463 779–89.
- 464 8. Snijdwind, I. J. M.; Van Kampen, J. J. a; Fraaij, P. L. a; Van der Ende, M. E.; Osterhaus, A. D.
465 M. E.; Gruters, R. a Current and future applications of dried blood spots in viral disease
466 management. *Antiviral research* **2012**, *93*, 309–21.
- 467 9. Denniff, P.; Spooner, N. The effect of hematocrit on assay bias when using DBS samples for
468 the quantitative bioanalysis of drugs. *Bioanalysis* **2010**, *2*, 1385–95.
- 469 10. Tanna, S.; Lawson, G. Analytical methods used in conjunction with dried blood spots.
470 *Analytical Methods* **2011**, *3*, 1709.
- 471 11. Holub, M.; Tuschl, K.; Ratschmann, R.; Strnadova, K. A.; Muehl, A.; Heinze, G.; Sperl, W.;
472 Bodamer, O. A. Influence of hematocrit and localisation of punch in dried blood spots on levels of
473 amino acids and acylcarnitines measured by tandem mass spectrometry. *Clinica Chimica Acta*
474 **2006**, *373*, 27–31.
- 475 12. Keevil, B. G. The analysis of dried blood spot samples using liquid chromatography tandem
476 mass spectrometry. *Clinical biochemistry* **2011**, *44*, 110–8.
- 477 13. Burnett, J. E. Dried blood spot sampling: practical considerations and recommendation for
478 use with preclinical studies. *Bioanalysis* **2011**, *3*, 1099–107.
- 479 14. Adam, B. W. J.; Alexander, R.; Smith, S. J.; Chace, D. H.; Loeber, J. G.; Elvers, L. H.;
480 Hannon, W. H. Recoveries of Phenylalanine from Two Sets of Dried-Blood-Spot Reference
481 Materials: Prediction from Hematocrit, Spot Volume, and Paper Matrix. *The American
482 Association for Clinical Chemistry* **2000**, *vol. 46*, 126–128.

- 483 15. Peng, M.; Liu, L.; Peng, L. Evaluation of factors influencing accuracy in the analysis of
484 succinylacetone in dried blood spots. *Clinica Chimica Acta* **2012**, *413*, 1265–1269.
- 485 16. Spooner, N.; Ramakrishnan, Y.; Barfield, M.; Dewit, O.; Miller, S. Use of DBS sample
486 collection to determine circulating drug concentrations in clinical trials: practicalities and
487 considerations. *Bioanalysis* 2010, *2*, 1515–22.
- 488 17. Alleborn, N.; Raszillier, H. Spreading and sorption of a droplet on a porous substrate.
489 *Chemical Engineering Science* **2004**, *59*, 2071–2088.
- 490 18. Kumar, S. M.; Deshpande, A. P. Dynamics of drop spreading on fibrous porous media.
491 *Colloids and Surfaces A: Physicochemical and Engineering Aspects* **2006**, *277*, 157–163.
- 492 19. Starov, V. . M.; Zhdanov, S. A.; Kosvintsev, S. R.; Sobolev, V. D. Spreading of liquid drops
493 over porous substrates. *Advances in Colloid and Interface Science* **2003**, *104*, 123–158.
- 494 20. Starov, V. M.; Kostvintsev, S. R.; Sobolev, V. D.; Velarde, M. G.; Zhdanov, S. a Spreading of
495 liquid drops over dry porous layers: complete wetting case. *Journal of colloid and interface*
496 *science* **2002**, *252*, 397–408.
- 497 21. Mei, J. V.; Alexander, J. R.; Adam, B. W.; Hannon, W. H. Use of Filter Paper for the Collection
498 and Analysis of Human Whole Blood Specimens. *The journal of nutrition* **2001**, 1631–1636.
- 499 22. Merrill, E. Rheology of blood. *Physiol. Rev* **1969**, *49*.
- 500 23. Baskurt, O. K.; Meiselman, H. J. Blood rheology and hemodynamics. *Seminars in thrombosis*
501 *and hemostasis* **2003**, *29*, 435–50.
- 502 24. O'Mara, M.; Hudson-Curtis, B.; Olson, K.; Yueh, Y.; Dunn, J.; Spooner, N. The effect of
503 hematocrit and punch location on assay bias during quantitative bioanalysis of dried blood spot
504 samples. *Bioanalysis* 2011, *3*, 2335–47.
- 505 25. O'Broin, S. Influence of Hematocrit on Quantitative Analysis of "Blood Spots" on Filter Paper.
506 *Clinical Chemistry* **1993**, *39*, 1354–1355.
- 507 26. Hoogtanders, K.; Van der Heijden, J.; Christiaans, M.; Edelbroek, P.; Van Hooff, J. P.; Stolk,
508 L. M. L. Therapeutic drug monitoring of tacrolimus with the dried blood spot method. *Journal of*
509 *pharmaceutical and biomedical analysis* **2007**, *44*, 658–64.
- 510 27. Clarke, A.; Blake, T.; Carruthers, K.; Woodward, A. Spreading and imbibition of liquid
511 droplets on porous surfaces. *Langmuir* **2002**, 2980–2984.
- 512 28. Windberger, U.; Bartholovitsch, A.; Plasenzotti, R.; Korak, K. J.; Heinze, G. Whole blood
513 viscosity, plasma viscosity and erythrocyte aggregation in nine mammalian species: reference
514 values and comparison of data. *Experimental physiology* **2003**, *88*, 431–440.
- 515 29. Baskurt, O. K. *Handbook of hemorheology and hemodynamics*; Baskurt, O. K.; Hardeman, M.
516 R.; Rampling, M. W.; Meiselman, H. J., Eds.; IOS Press, 2007; Vol. 69, pp. 1–455.
- 517 30. Thiriet, M. *Biology and Mechanics of Blood Flows. Part I: Biology*; Fieldman, J. S.; Saint-
518 Aubin, Y.; Phong, D. H.; Vinet, L., Eds.; Springer, 2007; p. 652.

519 31. Nassehi, V.; Das, D. B.; Shigidi, I. M. T. A.; Wakeman, R. J. Numerical analyses of bubble
520 point tests used for membrane characterisation : model development. *Asia Pacific Journal of*
521 *Chemical Engineering Engineering* **2011**, 850–862.

522 32. Semenov, S.; Trybala, A.; Rubio, R. G.; Kovalchuk, N.; Starov, V.; Velarde, M. G.
523 Simultaneous spreading and evaporation: Recent developments. *Advances in colloid and*
524 *interface science* **2013**.

525